FIELD ORIENTED CONTROL OF A BRUSHLESS DC MOTOR

A Project Report

submitted by

MARABATHINA HARSHAVARDHAN

in partial fulfilment of the requirements
for the award of the degree of

MASTER OF TECHNOLOGY

DEPARTMENT OF ELECTRICAL ENGINEERING
INDIAN INSTITUTE OF TECHNOLOGY MADRAS.

MAY 2017

THESIS CERTIFICATE

This is to certify that the thesis titled **FIELD ORIENTED CONTROL OF A BRUSHLESS DC MOTOR**, submitted by **Marabathina Harshavardhan**, to the Indian Institute of Technology, Madras, for the award of the degree of **Master of Technology**, is a bona fide record of the research work done by him under my supervision. The contents of this thesis, in full or in parts, have not been submitted to any other Institute or University for the award of any degree or diploma.

Dr. Srirama Srinivas
Project Guide
Associate Professor
Dept. of Electrical Engineering
IIT-Madras, 600036

Place: Chennai
Date: 12th May 2017

ACKNOWLEDGEMENTS

This project would not have been possible without the guidance and the help of several individuals who in one way or another contributed and extended their valuable assistance in the preparation and completion of this work.

First and foremost, my gratitude to Dr. Srirama Srinivas, Project Guide and Associate Professor, Dept. of Electrical Engineering, IIT Madras, whose sincerity and encouragement I will never forget. Dr. Srinivas has been my inspiration as I hurdle all the obstacles in the completion of this project. His guidance throughout the project was very helpful as he provided me with valuable suggestions and ideas, which helped me proceed towards my goal. Dr. Srinivas provided me an intellectual platform to enrich my knowledge and implement my views.

I am grateful to Mr. Ravi Teja Vallabhaneni, Research Scholar, without whose assistance this project would not have been successful. The discussions I had with him helped me to think in optimistic way. I am also thankful to Mr. Mariappan of Lucas-TVS for providing me with BLDC motor for my project.

Special thanks to Surya Prakash M, Siva Prasad K, Harikrishnan P and many others for their knowledge sharing in the time of need. I am also thankful to my friends Benny Sudhakar P, Subodhkanth K, Madhav Rao D, Chandra Kumar U, with whom I had most memorable time during my stay in IIT Madras.

ABSTRACT

KEYWORDS: Field Oiented Control; Sensored Control; SVPWM; BLDC

Brushless DC motors(BLDC) are widely used in present day applications due to their advantages over brushed DC motors.Field Oriented Control(FOC) of BLDC motors refers to a high performance control scheme which gives excellent dynamic torque and speed response similar to that of a DC machine. The present thesis encompasses the fundamentals of BLDC motor and the results and practical applications of FOC for BLDC motors. The primary focus in the work reported in this thesis is on controlling the motor in d-q axes using FOC technique along with the generation of space vector modulated pulses for the inverter driving the BLDC motor. This vector control method improves the system performance with low torque ripple and high efficiency.

TABLE OF CONTENTS

LIST OF TABLES

LIST OF FIGURES

ABBREVIATIONS

IITM	Indian Institute of Technology, Madras
BLDC	Brushless DC Motor
DSP	Digital Signal Processor
EMF	Electro Motive Force
PI	Proportional and Integral
DC	Direct Current
VSI	Voltage Source Inverter
FOC	Field Oriented Control
SVPWM	Space Vector Pulse Width Modulation
SPWM	Sine Pulse Width Modulation

NOTATION

v_a, v_b, v_c	Instantaneous voltages in *abc* frame, V
e_a, e_b, e_c	Instantaneous backEMFs in V
i_d, i_q	Instantaneous stator currents in *dq* frame, A
L_a, L_b, L_c	Stator inductances of three phases, mH
R_a, R_b, R_c	Stator resistances of three phases, Ω
M	Mutual inductance between any two phases, mH
V_{DC}	Inverter DC bus voltage, V
ω_m	Rotor speed, rad/s
K_p	Proportional gain of the PI controller
K_i	Integral gain of the PI controller

CHAPTER 1

INTRODUCTION

1.1 Brushed DC Motor

Brushed DC Motors are used in various adjustable speed drives due to their easier control, due to the fact that its speed and torque can be independently controlled from the field and current respectively. Stationary brushes are mounted to the stator frame which rub against commutator segments on the rotor, which in turn are connected to rotating coil segments. As the rotor spins, different coils are connected and disconnected in such a way that net magnetic field produced by rotor is stationary with respect to that of stator and properly oriented with stator magnetic field to produce the electromagnetic torque. As the commutator segments rotate past the brushes, the electrical contacts to those particular rotor coil segments will be broken. As the rotor coils are inductive, they oppose change in current by producing high fly-back voltage thereby causing sparks between brushes and disconnected commutator segments. These sparks results in several ill effects like reduced efficiency and calls for frequent replacement and for maintainance of the carbon brushes etc. The brushes must be spring loaded against commutator segments in order to ensure good electrical contact. This further reduces efficiency and periodic maintenance to replace the brushes.

1.2 Brushless DC Motor

In the past few years, the field of controlled electrical drives has undergone rapid expansion due to technological improvements in semiconductor devices. New electronic microprocessors and DSPs which provide amazing computational speeds have enabled

the development of effective vector control AC drives with lower power dissipation and more accurate control. BLDC motors are one of the motor types rapidly gaining popularity. BLDC motors are used in industries such as appliances, automotive, aerospace, consumer, medical, industrial automation equipment and instrumentation. As the name implies, BLDC motors do not use brushes for commutation; instead, they are electronically commutated. BLDC motors have many advantages over brushed DC motors and induction motors.A few of these are:

1. Better speed versus torque characteristics
2. High dynamic response
3. Higher speed ranges
4. Long operating life
5. High efficiency
6. Less noise operation

In addition, there are no brushes and commutator in the motor and therefore all disadvantages associated with sparking of brushed DC motors are eliminated.

1.3 Construction of BLDC motor

BLDC motor is a type of permanent magnet synchronous machine. The motor has 3-phase delta connected or star connected stator and the rotor has permanent magnets.

1.3.1 Stator

The stator of a BLDC motor consists of stacked steel laminations with windings placed in the slots that are axially cut along the inner periphery. The stator resembles that of an induction motor; however, the windings are distributed in a different manner. Most BLDC motors have three stator windings connected in star or delta fashion. Each of these windings are constructed with numerous coils interconnected to form a winding. One or more coils are placed in the slots and they are interconnected to make a winding.

Each of these windings are distributed over stator periphery to form an even number of poles. There are two types of stator winding variants: trapezoidal and sinusoidal motors. This differentiation is based on the basis of interconnection of coils in the stator windings to give different types of back emf. The trapezoidal motor gives a back emf in trapezoidal fashion and sinusoidal motors back emf is sinusoidal.

1.3.2 Rotor

The rotor is made up of permanent magnets. Permanent magnet synchronous machines can be broadly classified on the basis of the direction of field flux.

1. Radial field: The flux direction is along the radius of the machine.
2. Axial field: The flux direction is parallel to the rotor shaft.

The magnets can be placed in many ways on the rotor. The high power density synchronous machines have surface mounted permanent magnets with radial orientation intended generally for low speed applications whereas in interior magnet version, the permanent magnets are inset and are used for high speed applications. The airgap flux is ideally decided by the magnets and little affected by armature current.

1.3.3 Hall Sensors

The commutation of a BLDC motor is controlled electronically. In BLDC motor, the stator windings should be energized in a particular sequence to rotate in a particular direction. It is important to know the rotor position in order to understand which winding must be energized, following the energizing sequence. Rotor position is sensed using Hall sensors embedded in stator. Most BLDC motors have three Hall sensors embedded into stator on non-driving end of motor. Whenever the rotor magnetic poles pass near Hall sensors, they give a high or low signal, indicating the N or S pole is passing near the sensors. Based on the combination of these Hall sensor signals, the exact sequence of commutation can be determined.

1.4 Operating Principle

Trapezoidal BLDC motor is a type of permanent magnet synchronous motor that has a trapezoidal shaped back-emf. DC power supply switched to stator phase windings of motor using power devices is given, where the switching sequence is determined from the rotor position. The phase current, typically rectangular in shape, is synchronized with the back-emf to produce a constant torque at constant speed. BLDC motors are commutated using a three phase inverter which requires rotor position information. The position of rotor can be sensed by using hall sensors, resolvers or obsolute position sensors. BLDC motors come in single phase, two phase and three phase configurations. Corresponding to its type, the stator has same number of windings. Out of these, three phase motors are most popular and widely used. A typical three phase inverter connected to a three phase BLDC motor equivalent circuit is shown in Figure. 1.1.

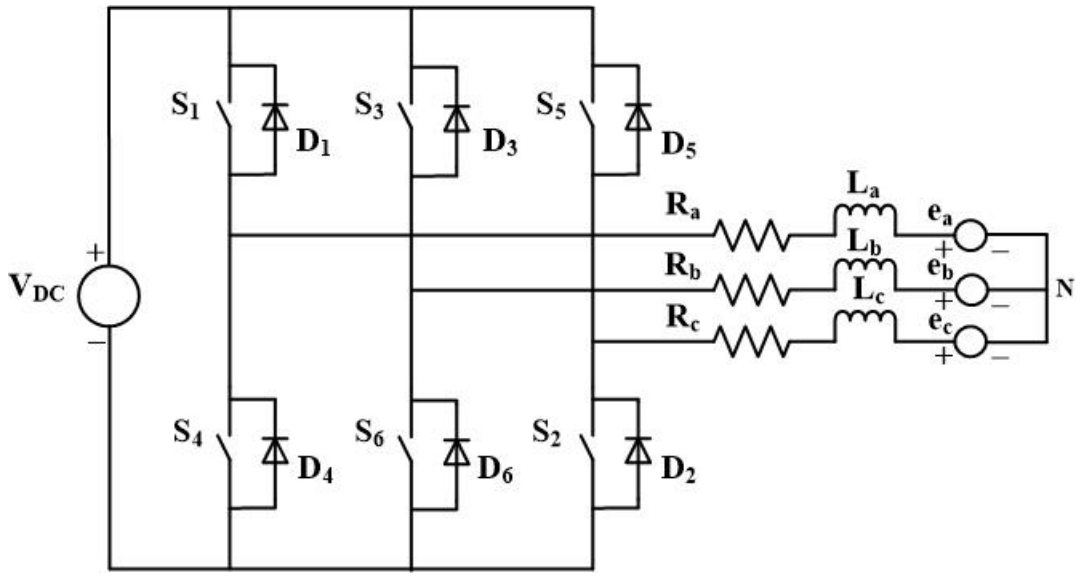

Figure 1.1: Three Phase BLDC motor fed from a 3ϕ voltage source inverter

Typically, a BLDC motor is driven by a three phase inverter with six step commutation. The conducting interval for each phase is 120^0 electrical angle and each conducting state is called a step. Each commutation sequence has one of the windings energized to the positive DC supply of the inverter(current flows into the winding) and the second winding to the negative DC supply of the inverter(current flows out of winding) and

the third winding is in non-energized condition. The interaction of magnetic fields produced by stator coils and permanent magnets produces a constant torque. In order to produce maximum torque, the inverter should be commutated every 60^0 so that current is in phase with back-emf. The ideal back-emf waveforms of the three phases along with phase currents is shown in Figure. 1.2. Table 1.1 shows the switching sequence that should be followed with respect to Hall sensors.

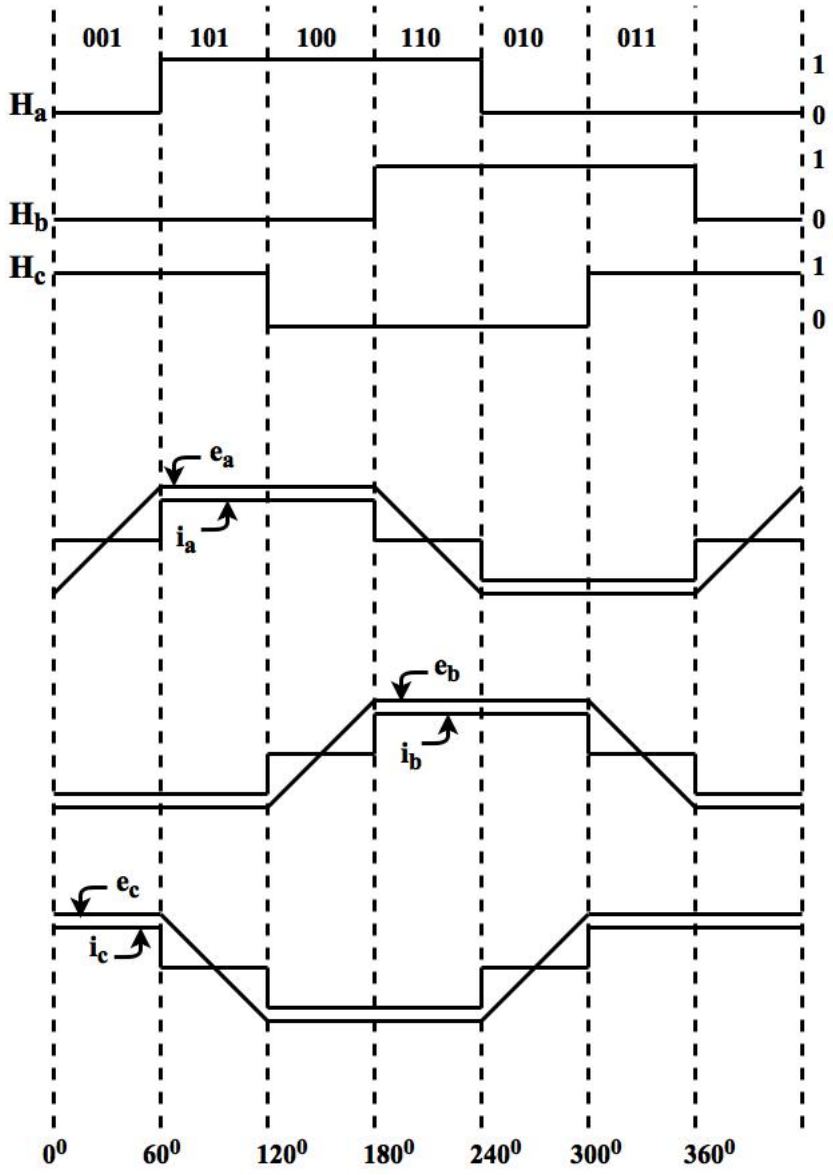

Figure 1.2: Ideal back EMF's, phase currents and hall sensor signals

Rotor Position	H_a	H_b	H_c	S_1	S_2	S_3	S_4	S_5	S_6	Phases which are ON
0^0-60^0	0	0	1	0	0	0	0	1	1	CB
60^0-120^0	1	0	1	1	0	0	0	0	1	AB
120^0-180^0	1	0	0	1	1	0	0	0	0	AC
180^0-240^0	1	1	0	0	1	1	0	0	0	BC
240^0-300^0	0	1	0	0	0	1	1	0	0	BA
300^0-360^0	0	1	1	0	0	0	1	1	0	CA

Table 1.1: Hall sensor signals showing switching sequence

1.5 Organization of the Report

• Chapter 2 deals with mathematical modelling of Brushless Dc motor and gives details about the operation of BLDC motor using hall sensors in MATLAB-Simulink and in Hardware.

• Chapter 3 explains the theory of Field Oriented Control, SVPWM, Design of controllers and displayed various simulation results.

• Chapter 4 gives the conclusions and the future scope of the project.

CHAPTER 2

MATHEMATICAL MODELLING OF BLDC MOTOR AND OPERATION OF BLDC MOTOR USING HALL SENSORS

2.1 Model of BLDC motor

The BLDC motor is represented by a three-phase equivalent circuit, where each phase consists of stator resistance, self inductance, and a trapezoidal backemf in series.

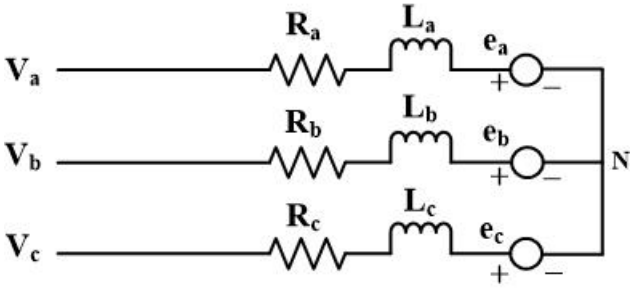

Figure 2.1: Model of BLDC motor

The voltage equations of the three phases can be written as

$$v_a = R_a i_a + \frac{d}{dt}(L_a i_a + L_{ba} i_b + L_{ca} i_c) + e_a \tag{2.1}$$

$$v_b = R_b i_b + \frac{d}{dt}(L_{ab} i_a + L_b i_b + L_{cb} i_c) + e_b \tag{2.2}$$

$$v_c = R_c i_c + \frac{d}{dt}(L_{ac} i_a + L_{bc} i_b + L_c i_c) + e_c \tag{2.3}$$

We have

$$R_a = R_b = R_c = R$$

$$L_a = L_b = L_c = L_s$$

$$L_{ba} = L_{ab} = L_{ca} = L_{ac} = L_{bc} = L_{cb} = M$$

Substituting above values, (2.1) - (2.3) can be written in the matrix form as ;

$$\begin{bmatrix} v_a \\ v_b \\ v_c \end{bmatrix} = \begin{bmatrix} R & 0 & 0 \\ 0 & R & 0 \\ 0 & 0 & R \end{bmatrix} + L \begin{bmatrix} \frac{di_a}{dt} \\ \\ \frac{di_b}{dt} \\ \\ \frac{di_c}{dt} \end{bmatrix} + \begin{bmatrix} e_a \\ e_b \\ e_c \end{bmatrix} \tag{2.4}$$

where,

$L_s - M = L$

R is stator resistance per phase

L_s is stator inductance per phase

M is mutual inductance between the phases

i_a, i_b, i_c are the stator currents per phase

The amplitude of back-emf depends on speed and its waveform depends on the rotor position. Also, the back-emf waveforms have 120^0 phase difference between each phase. Therefore, back-emf can be mathematically written as ;

$$e_a = k_b(\theta_e)\omega_r \tag{2.5}$$

$$e_b = k_b(\theta_e - \frac{2\pi}{3})\omega_r \tag{2.6}$$

$$e_c = k_b(\theta_e + \frac{2\pi}{3})\omega_r \tag{2.7}$$

where,

ω_r is rotor mechanical speed in *rad/s*

θ_e is rotor electrical position in *rad*

k_b is back EMF constant which is dependent on rotor position and expressed in V/*rad/s*

The electro-magnetic torque developed in the machine can be written as

$$T_e = \frac{e_a i_a + e_b i_b + e_c i_c}{\omega_r} \tag{2.8}$$

The equation of motion is

$$T_e - T_l = J\frac{d\omega_r}{dt} + B\omega_r \tag{2.9}$$

Where,

J is Moment of inertia[kgm^2]

B is Coefficient of friction[*Nms/rad*]

T_l is Load torque[*Nm*]

2.2 Theory of Operation

Unlike Brushed DC motor, commutation of BLDC motor is controlled electronically. To rotate BLDC motor, the stator windings should be energized in a sequence. It is important to know the rotor position in order to understand which winding to be energized following the energizing sequence. The rotor position is sensed using hall sensors embedded into the stator. Most BLDC motors have three hall sensors embedded into stator at their non-driving end of the rotor. Whenever the rotor magnetic poles pass near hall sensors, they give a high or low signal, indicating the N or S pole is passing near the hall sensor. Based on the combination of the three hall sensor signals, the exact sequence of commutation is determined.

Every 60^0 electrical rotation of rotor, one of the hall sensors changes its state. Given this, it takes six steps to complete one electrical cycle. In synchronous with every 60^0

electrical, phase current switching should be updated. However, one electrical cycle may not correspond to one mechanical revolution of the rotor. The number of cycles to be repeated to complete a mechanical rotation is determined by number of rotor pole pairs. For each rotor pole pair, one electrical cycle is completed. So, the number of electrical cycles per revolution is equal to rotor pole pairs.

2.3 Simulation Results

Using (2.1) to (2.9), the BLDC motor is modelled in MATLAB-simulink. The supply to the motor is taken from a three phase inverter as shown in Figure. 2.2. Three stator windings are modelled using resistance, inductance and a voltage controlled source which is driven by ideal back-emf waveforms derived from the speed of motor and rotor angle. Currents in each phase are used to calculate the total electro-magnetic torque from which speed is calculated. Three hall sensor signals are also derived from the rotor position.

The parameters of the motor used for simulation are shown in Table 2.1.

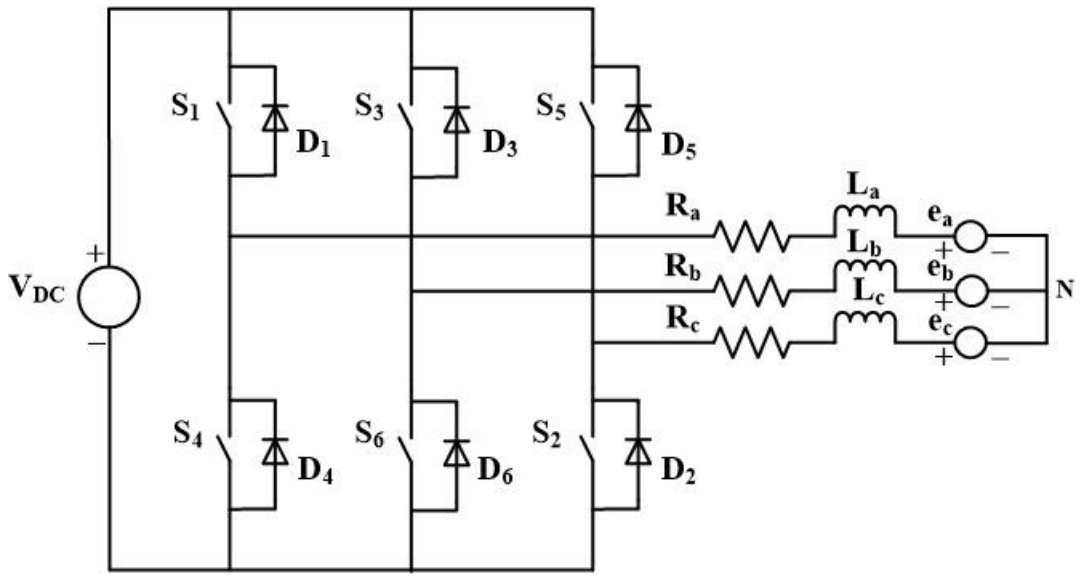

Figure 2.2: 3ϕ voltage source inverter fed BLDC motor

The induced back-emf and phase current of A-phase at the time of starting are shown in Figure. 2.3 and 2.4 respectively. From Figure. 2.4 it can be seen that the motor draws

Table 2.1: BLDC motor parameters used for simulation

Parameter	Value	Units
Resistance	3.5	ohms
Inductance	19	mH
DC Voltage	48	Volts
Voltage constant	98.03	V_{peak} L-L / krpm
No.of poles	16	

a high starting current since there is no induced back-emf. As the motor rotates and speed picks up, the back-emf increases and hence current drawn by the motor decreases which can be seen from Figure. 2.5 and Figure. 2.6 respectively.

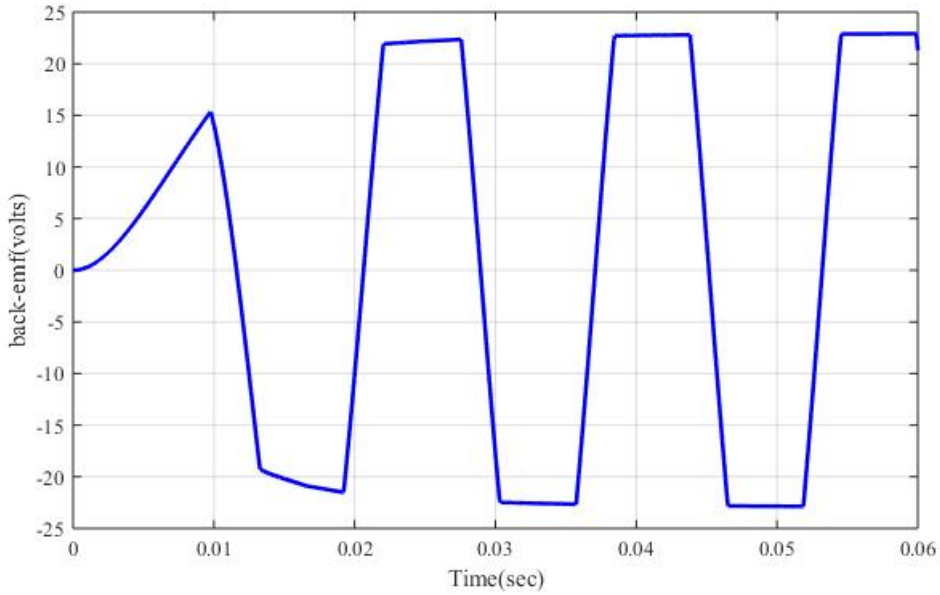

Figure 2.3: Induced EMF e_a at starting

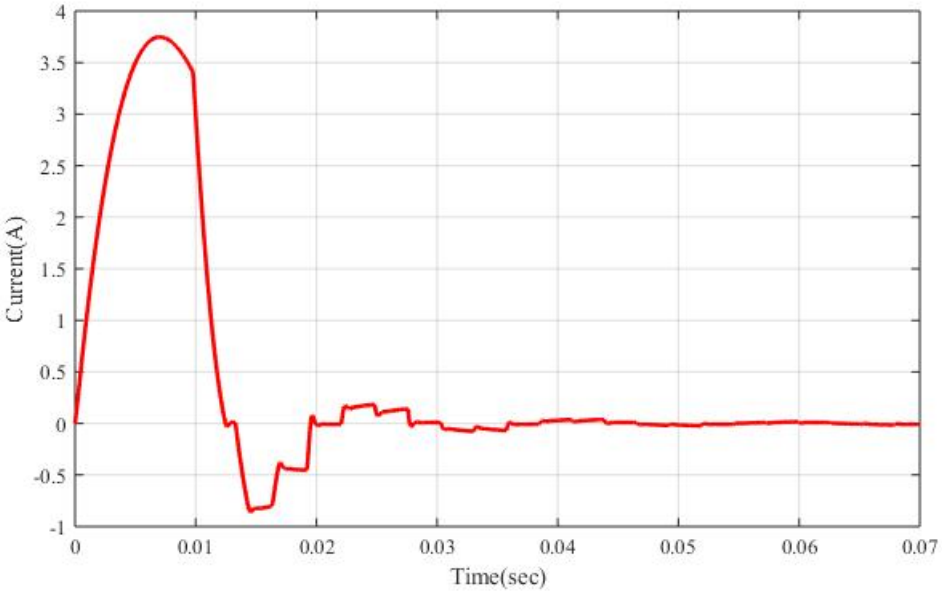

Figure 2.4: Phase current i_a at starting

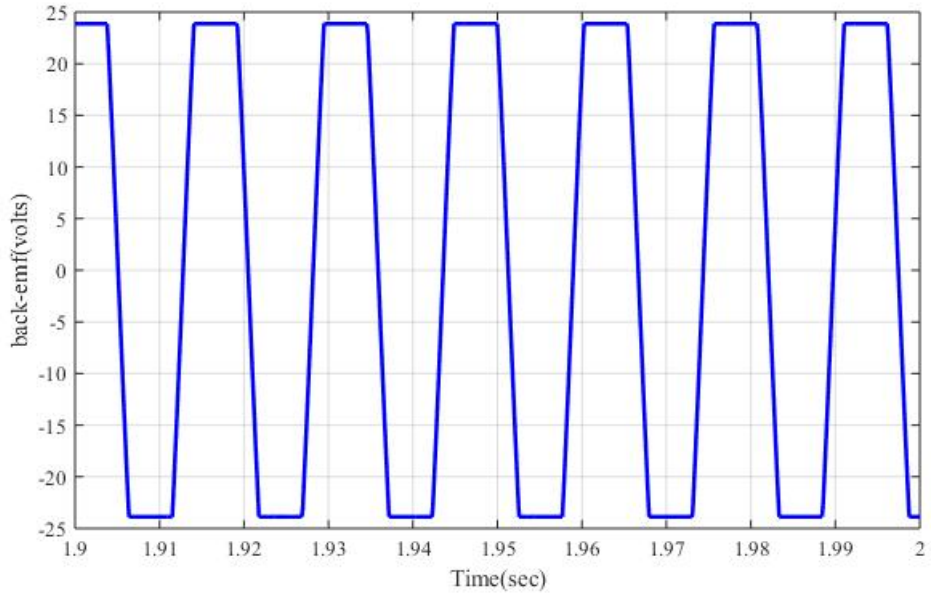

Figure 2.5: Induced EMF e_a during staedy state

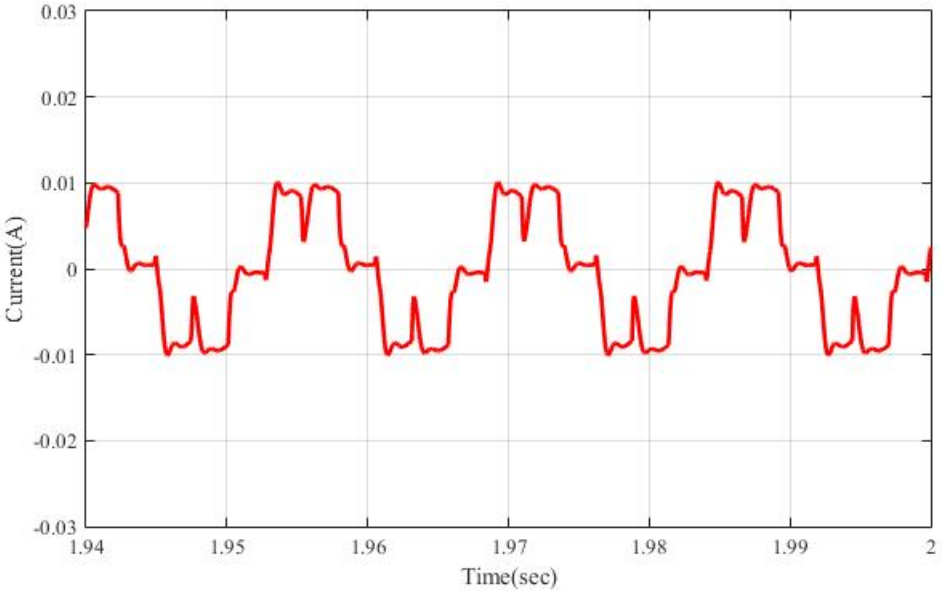

Figure 2.6: Phase current i_a during steady state

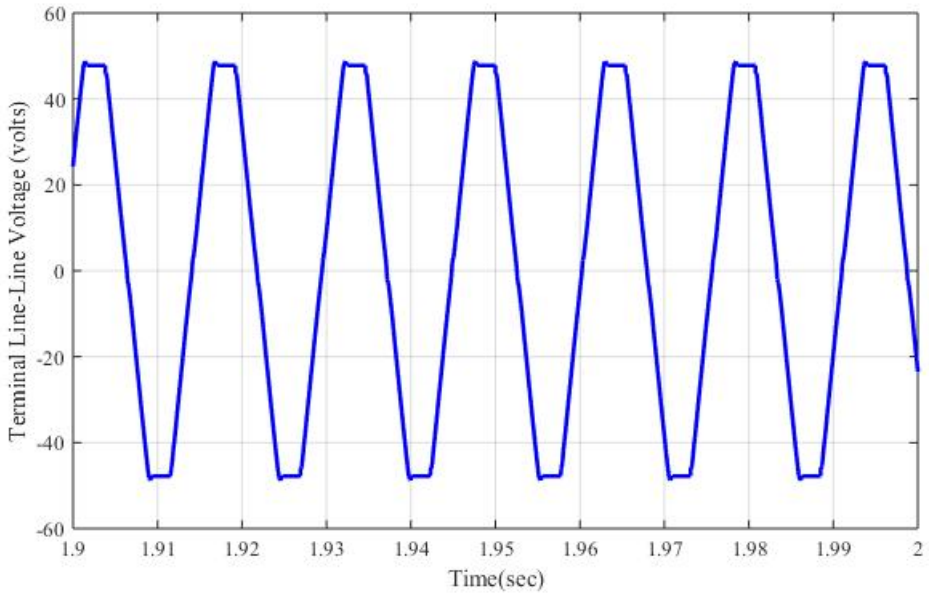

Figure 2.7: Terminal voltage V_{ac}

The terminal line-line voltage V_{ac} is shown in Figure. 2.7 and the BLDC motor speed and torque waveforms are shown in Figure. 2.8 and Figure. 2.9 respectively. From Figure. 2.9 it can be seen that starting torque will be high due to high current drawn by the BLDC motor and the BLDC motor speed settles down at steady state at which the electromagnetic torque developed by the motor equals the load torque.

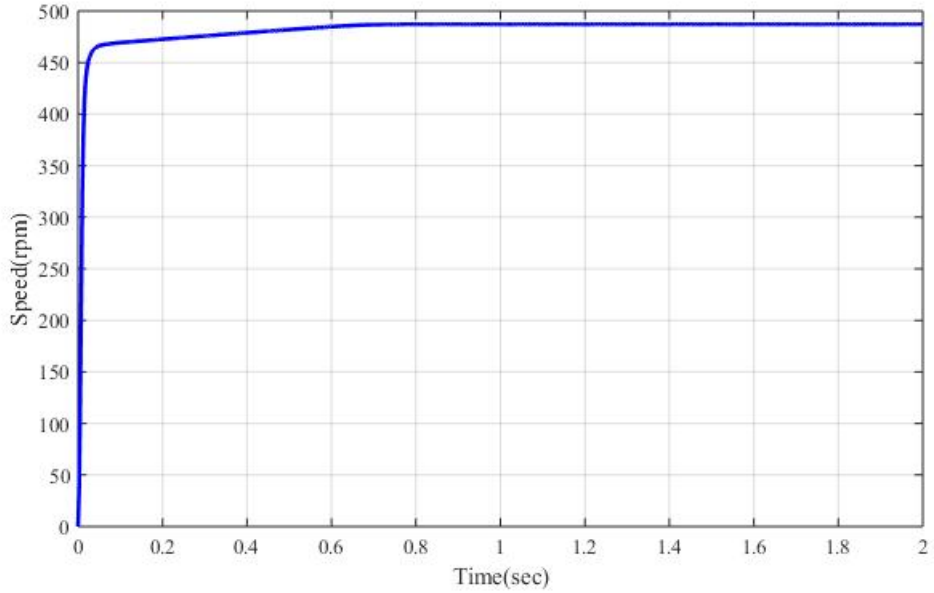

Figure 2.8: Speed of the motor

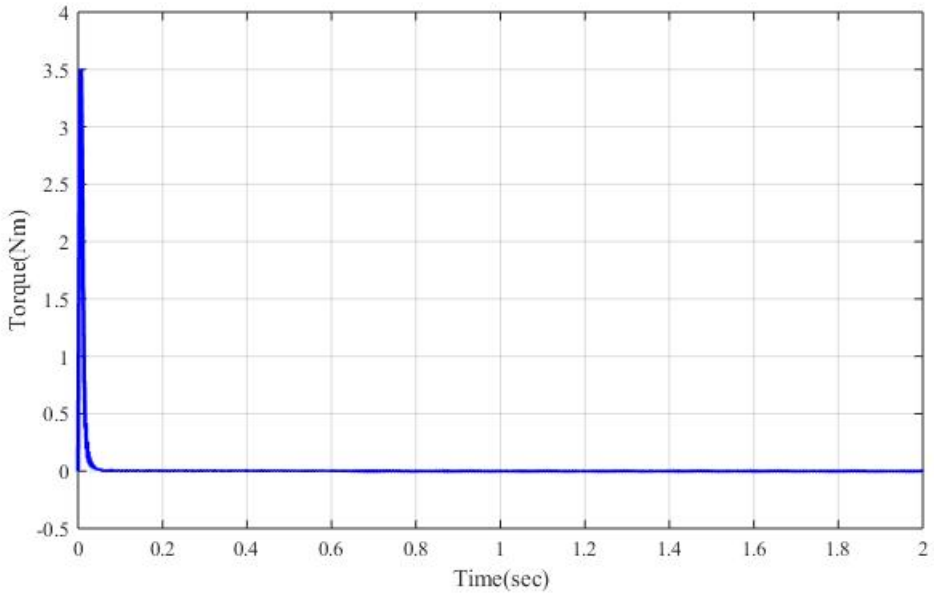

Figure 2.9: Electro-magnetic Torque T_e

2.4 Experimental Results

The specifications of the BLDC motor used for the experiment are shown in Table 2.2. The hardware setup of the experiment is shown in Figure. 2.10. The level shifter board

and DSP is shown in Figure. 2.11. Hall sensors require 0-5V supply for its operation.

Table 2.2: Motor parameters used for experimental procedure

Parameter	Value	Units
Resistance	3.5	ohms
Inductance	19	mH
DC Rated Voltage	48	Volts
No.of poles	16	

Figure 2.10: Hardware Setup

The hall sensor outputs are given to the TMS320F28377S digital control platform. The coding of DSP is done by using embedded MATLAB coder. DSP board requires a 3.3V supply and ground connection for its operation. The code is developed to give six outputs that depend on the combination of three hall sensor outputs which decide the control signals for switching the semiconductor switches of the three-phase inverter drive. The gate driver requires 15V supply for its operation. Therefore, gate pulses coming out from DSP control platform are needed to be level shifted from 3.3V to 15V. CD4504B Hex Voltage-Level shifter is used for this operation. The commutation sequence of switches and phases in conduction according to hall sensor outputs are given in Table 2.3. In Table 2.3, a '1' indicates ON state of switch and a '0' indicates OFF state. Also a 'A+' refers to top switch of phase A and a 'A-' its bottom switch.

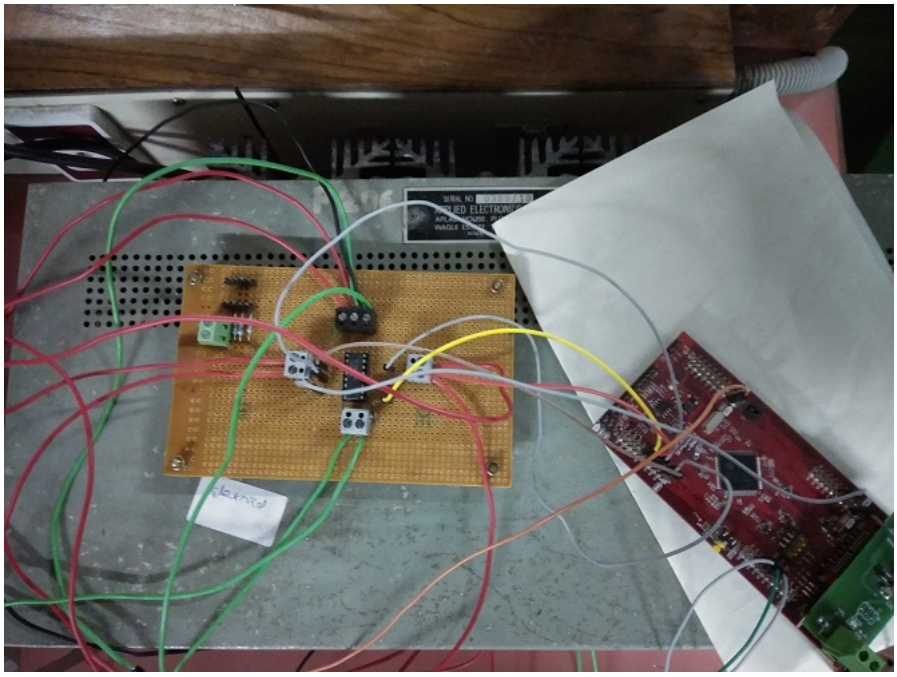

Figure 2.11: Levelshifter Circuit

Table 2.3: Commutation sequence derived from hall sensor outputs

H_a	H_b	H_c	S1	S2	S3	S4	S5	S6	Phases in conduction
0	0	1	0	0	0	0	1	1	C+,B-
1	0	1	1	0	0	0	0	1	A+,B-
1	0	0	1	1	0	0	0	0	A+,C-
1	1	0	0	1	1	0	0	0	B+,C-
0	1	0	0	0	1	1	0	0	B+,A-
0	1	1	0	0	0	1	1	0	C+,A-

Similarly for B and C phases also.

The stator of the BLDC motor is connected in star. The three hall sensor outputs are obtained and they are shown in Figure. 2.12.

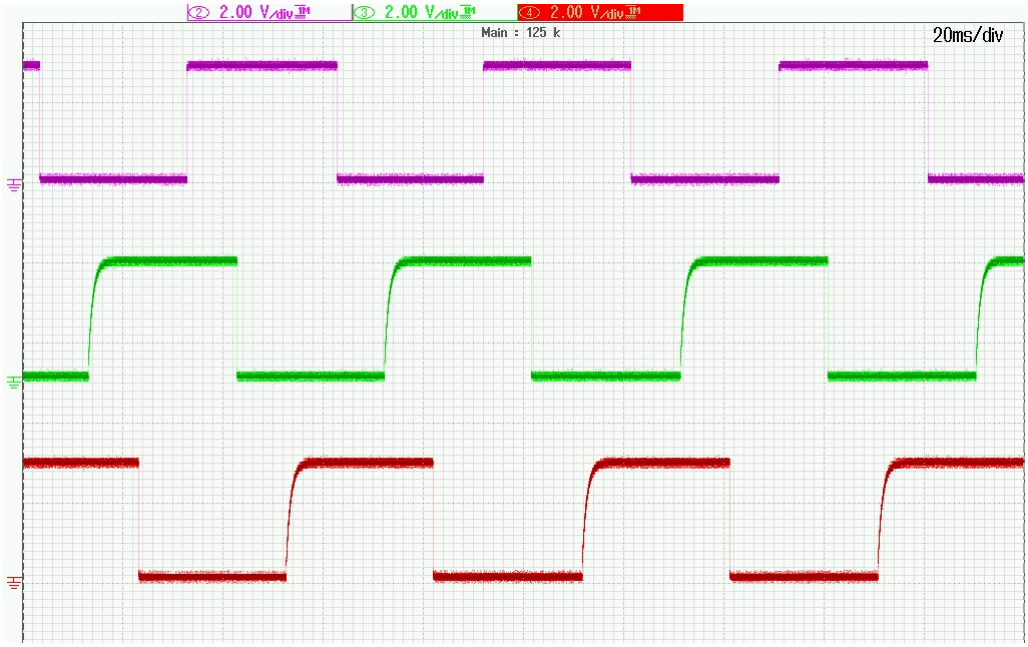

Figure 2.12: Three Hall sensor signal Waveforms

The waveforms of pulses coming from DSP have 3.3V and are level-shifted. The level-shifted pulses given to gate driver i.e at 15V are shown in Figure. 2.13 and Figure. 2.14 respectively.

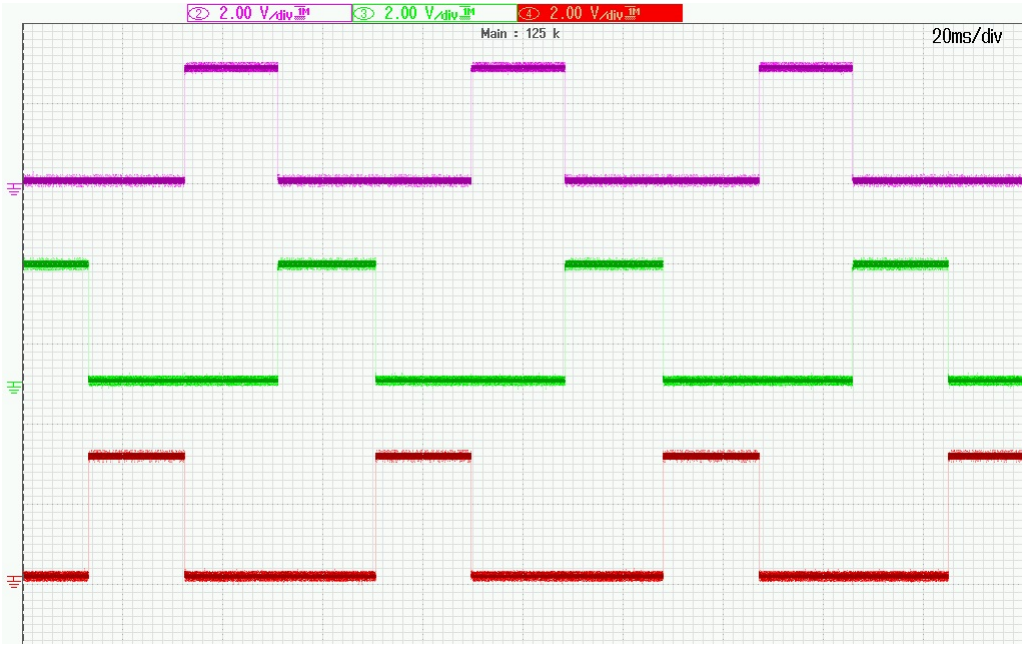

Figure 2.13: Pulses coming out from DSP

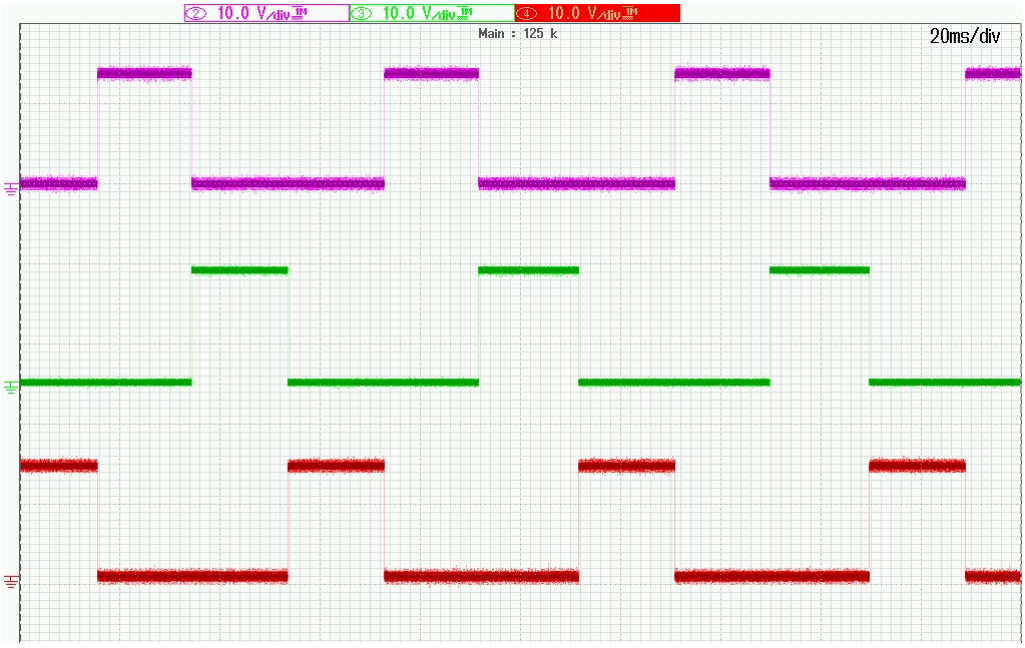

Figure 2.14: Pulses given to Gate driver

The phase current waveform of A phase is shown in Figure. 2.15. The terminal line-line voltage is measured by using 100:1 high voltage probe and the waveform is shown in Figure. 2.16.

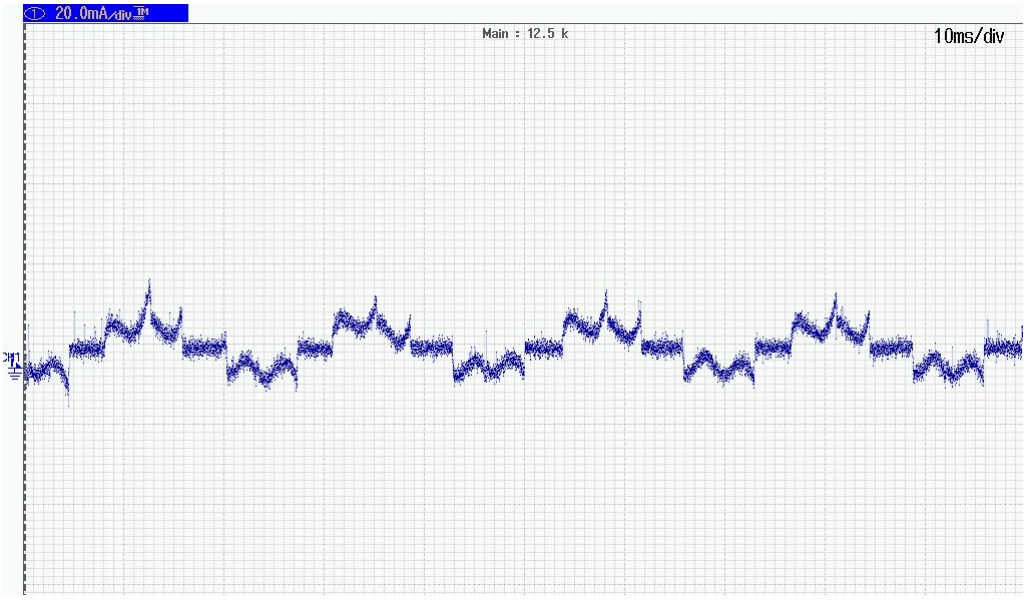

Figure 2.15: Phase current waveform

The rated speed of BLDC motor calculated from Figure. 2.8 is 487rpm and the rated speed of BLDC motor calculated from the experiment is 500rpm. The peak value of

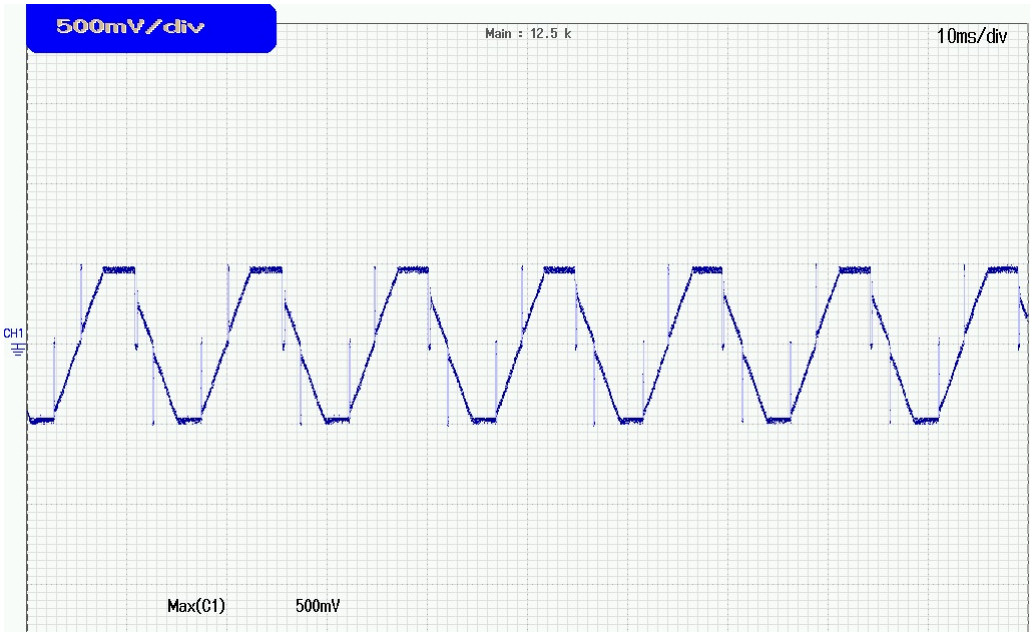

Figure 2.16: Line-Line terminal voltage waveform

the phase current calculated from the Figure. 2.15 is 12mA and the maximum value of current calculated from the Figure. 2.6 is 10mA. The peak value of terminal line-line voltage calculated from the Figure. 2.16 is 50V and the maximum value of terminal line-line voltage calculated from the Figure. 2.7 is 48V.

CHAPTER 3

FIELD ORIENTED CONTROL OF BLDC MOTOR

3.1 Theory of Field Oriented Control

In trapezoidal current control, the BLDC motor operates in two phase conduction mode. In SVPWM based field oriented control, the BLDC motor operates in three phase conduction mode and this results in sinusoidal currents. The BLDC motor is modelled in three phase stator reference frame and the transformations from three phase stator reference frame to d-q rotating reference frame are done by using clarke and park transformations. In FOC, motor currents and voltages are manipulated in the d-q reference frame of the rotor. This means that measured motor currents must be mathematically transformed from the three-phase static reference frame of the stator windings to the two axis rotating d-q reference frame, prior to processing by the PI controllers. Similarly, the voltages to be applied to the motor are transformed from the dq frame of the rotor to the three phase reference frame of the stator before they can be used for SVPWM output as shown in Figure. 3.1. These transformations generally require the fast math capability of a DSP or high performance digital signal processing power that becomes the heart of FOC. Although the reference frame transformations can be performed in a single step, they are best described as a two step process. The motor currents are first translated from the 120 degree physical frame of the motor stator windings to a fixed orthogonal reference frame. They are then translated from the stator fixed frame to the rotating frame of the rotor. Two P-I controllers are used; one for the direct current component, and the other for the quadrature current. The input to the controller for the direct current has zero input. This drives the direct current component to zero and therefore forces the current space vector to be exclusively in the quadrature direction. Since only the quadrature current produces useful torque, this maximizes the torque

efficiency of the system. The second P-I controller operates on quadrature current and takes the requested torque as input. This causes the quadrature current to track the requested torque, as desired. The outputs from the two P-I controllers represent a voltage space vector with respect to the rotor. Mirroring the transformation performed on motor currents, these static signals are processed by a series of reference frame transformations to produce voltage control signals for the output bridge. They are first translated from the rotating d-q frame of the rotor to the fixed x-y frame of the stator. The voltage signals are then converted from an orthogonal frame to the 120 degree physical frame of the A, B and C motor windings. This results in three voltage signals appropriate for control of the SVPWM output modulator.

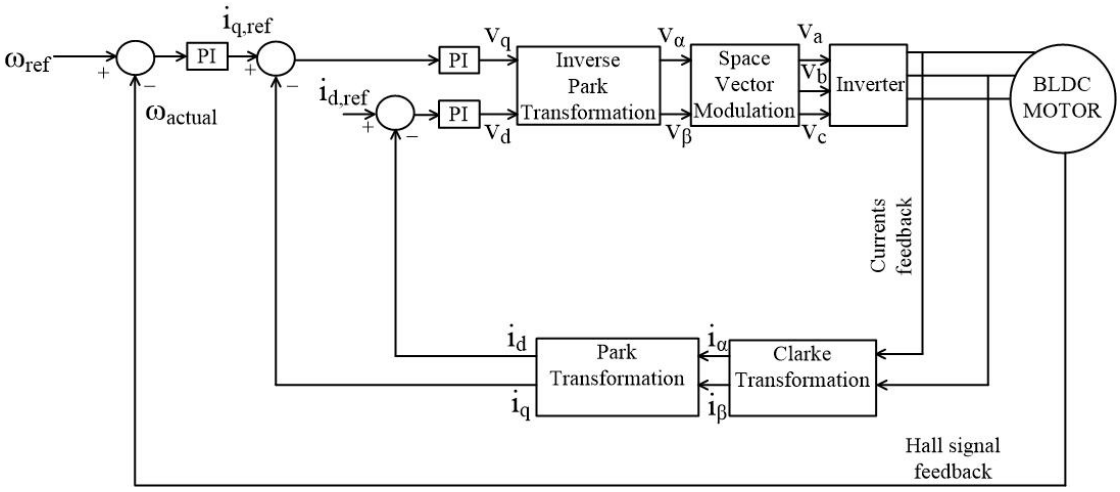

Figure 3.1: Block diagram of Field Oriented control

3.2 SVPWM switching for inverter

The power circuit topology for a 2-level VSI using IGBT switches is shown in Figure. 3.2.For this inverter, there are 8 possible combinations of switching. Each of the switching combination results in a space vector wose location can be obtained. Of these, two are zero vectors that corresponding to all top switches or all bottom switches ON. The other six vectors are directed along the vertices of a regular hexagon giving six sectors S_1 - S_6 as shown in Figure. 3.3.

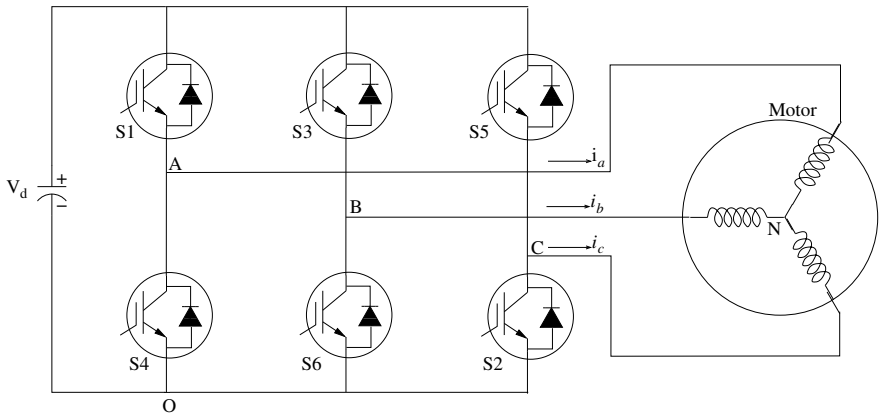

Figure 3.2: 2-level VSI topology

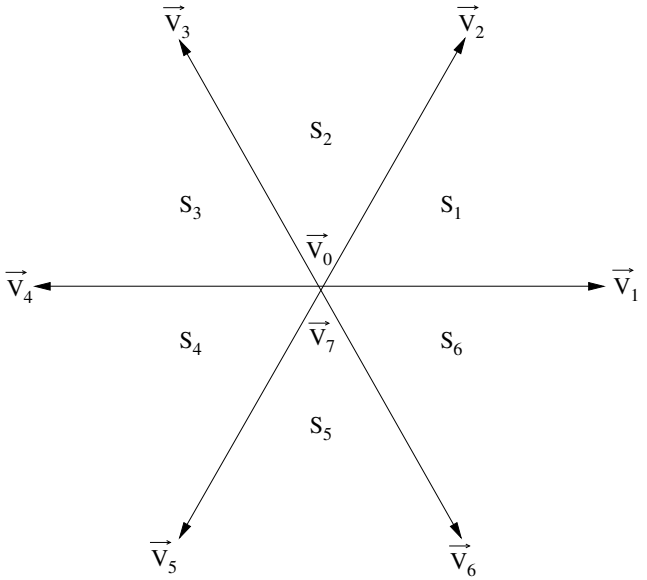

Figure 3.3: Space vector locations for the 2-level VSI

The various possible switching combinations, along with their corresponding space vector locations and the components of these vectors along the α and β axes are listed in Table. 3.1. In Table 3.1 a '0' corresponds to the switch being OFF and a '1' corresponds to the switch being ON.

Table 3.1: Space vectors for different switching states

S_1	S_3	S_5	V_{AN}	V_{BN}	V_{CN}	Vector	V_α	V_β
0	0	0	0	0	0	$\overrightarrow{V_0}$	0	0
1	0	0	$2V_d/3$	$-V_d/3$	$-V_d/3$	$\overrightarrow{V_1}$	$2V_d/3$	0
0	1	0	$-V_d/3$	$2V_d/3$	$-V_d/3$	$\overrightarrow{V_3}$	$-V_d/3$	$V_d/\sqrt{3}$
1	1	0	$V_d/3$	$V_d/3$	$-2V_d/3$	$\overrightarrow{V_2}$	$V_d/3$	$V_d/\sqrt{3}$
0	0	1	$-V_d/3$	$-V_d/3$	$2V_d/3$	$\overrightarrow{V_5}$	$-V_d/3$	$-V_d/\sqrt{3}$
1	0	1	$V_d/3$	$-2V_d/3$	$V_d/3$	$\overrightarrow{V_6}$	$V_d/3$	$-V_d/\sqrt{3}$
0	1	1	$-2V_d/3$	$V_d/3$	$V_d/3$	$\overrightarrow{V_4}$	$-2V_d/3$	0
1	1	1	0	0	0	$\overrightarrow{V_7}$	0	0

The fundamental idea of SVPWM is that a given reference vector can be realised in the average sense using the combination of the eight space vectors of the 2-level VSI. The reference voltage vector is obtained by mapping the desired 3-ϕ output voltages to the $\alpha\beta$ frame. It is then realised by using the vectors that form the boundary of the sector in which the tip of the reference vector lies. Figure. 3.4 illustrates this technique for a vector that lies in sector 1.

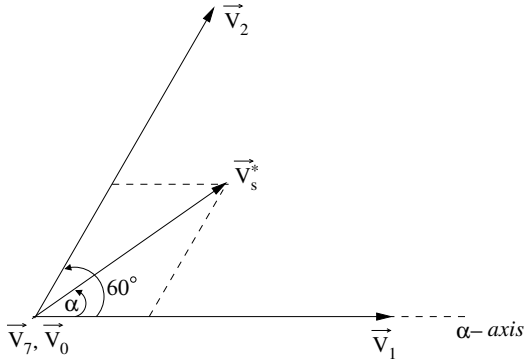

Figure 3.4: Synthesising a desired reference vector by SVPWM

For any sampling interval T_s, during which the desired vector lies in sector-1 as shown in Figure. 3.4, the sampling interval is divided into 3 sub intervals i.e T_1, T_2 and T_0. The switching is done to obtain the vector $\vec{V_1}$ for T_1 seconds, $\vec{V_2}$ for T_2 seconds and any of the zero vectors for T_0 seconds. The intervals T_0, T_1 and T_2 are chosen such that volt seconds produced by the active vectors and the zero vector along the α and β axis,

are the same as that produced by v_s^* in the total sampling time interval T_s. Therefore,

$$|V_s^*|T_s \cos\alpha = T_1|\vec{V_1}| + T_2|\vec{V_2}| \cos 60^\circ \quad (3.1)$$

$$|V_s^*|T_s \sin\alpha = T_2|\vec{V_2}| \sin 60^\circ \quad (3.2)$$

Solving for T_1 and T_2 and defining the modulation index as $m = \frac{|\vec{V_s^*}|}{|\vec{V_1}|}$ gives

$$T_1 = mT_s \frac{\sin(60^\circ - \alpha)}{\sin 60^\circ} \quad (3.3)$$

$$T_2 = mT_s \frac{\sin\alpha}{\sin 60^\circ} \quad (3.4)$$

$$T_0 = T_s - T_1 - T_2 \quad (3.5)$$

In (3.3) and (3.4) the angle α is the angle subtended by the reference space vector with respect to α-axis in Figure. 3.4 and this is easily obtained from the components along the α and β axis. Since the same equations apply to any sector, only a 60° sine lookup table is required. The switching pattern used in this project using vectors in sector S_1 is as shown in Figure. 3.5.

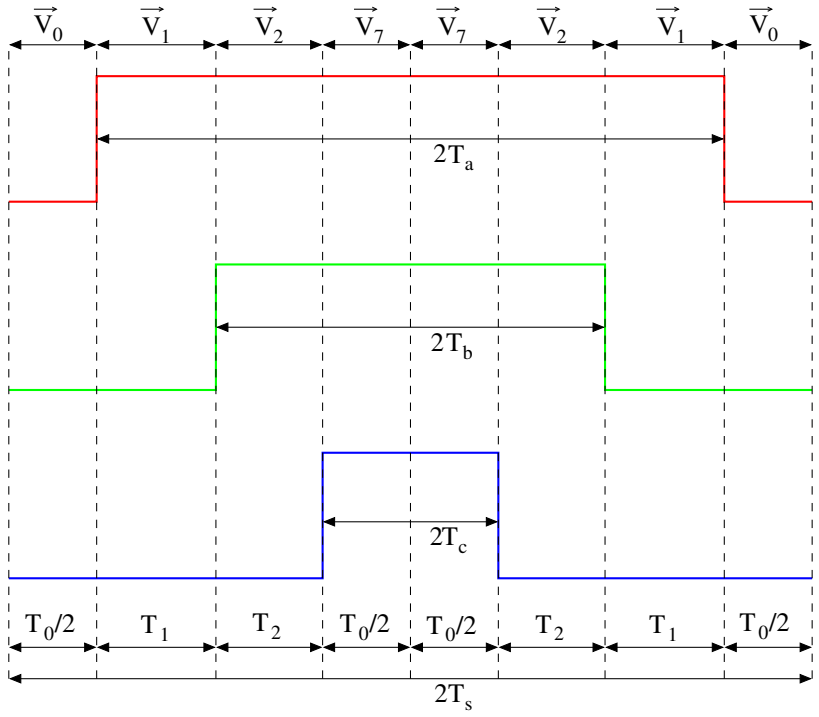

Figure 3.5: Switching pattern for 2 succesive sampling intervals

For this pattern it can be seen that,

$$\begin{aligned} T_c &= T_0/2 \\ T_b &= T_2 + T_0/2 \\ T_a &= T_s - T_0/2 \end{aligned}$$

Similarly for other sectors, T_a, T_b, T_c values can be calculated and is shown in Table. 3.2

Table 3.2: T_a, T_b, T_c values for different sectors

Sector	S_1	S_2	S_3	S_4	S_5	S_6
T_a	T_s-T_0/2	T_1 + T_0/2	T_0/2	T_0/2	T_2+T_0/2	T_2+T_0/2
T_b	T_2 + T_0/2	T_s - T_0/2	T_s - T_0/2	T_1+T_0/2	T_0/2	T_0/2
T_c	T_0/2	T_0/2	T_2 + T_0/2	T_s-T_0/2	T_s-T_0/2	T_1+T_0/2

3.3 Design of Current and Speed controllers

3.3.1 Current controller

Current controllers primarily deal with the dynamics of the power supply and armature. These should have a response slower than the inverter, but faster than the speed controller. The block diagram of the current controller loop is as shown in Figure. 3.6. The structure of q-axis current controller is also same. If the bandwidth of current controller is chosen as f_n Hz, then

$$t_b = \frac{1}{2\pi f_n} \tag{3.6}$$

The bandwidth of current controller loop = $f_n = \frac{1}{10} \times$Bandwidth of inverter
The condition for the loop to have a first order response is

$$t_{cc} = \frac{L}{R} \tag{3.7}$$

Therefore, the open loop gain is

$$\frac{k_{pc}}{R.t_{cc}.s} = \frac{1}{s.t_b} \tag{3.8}$$

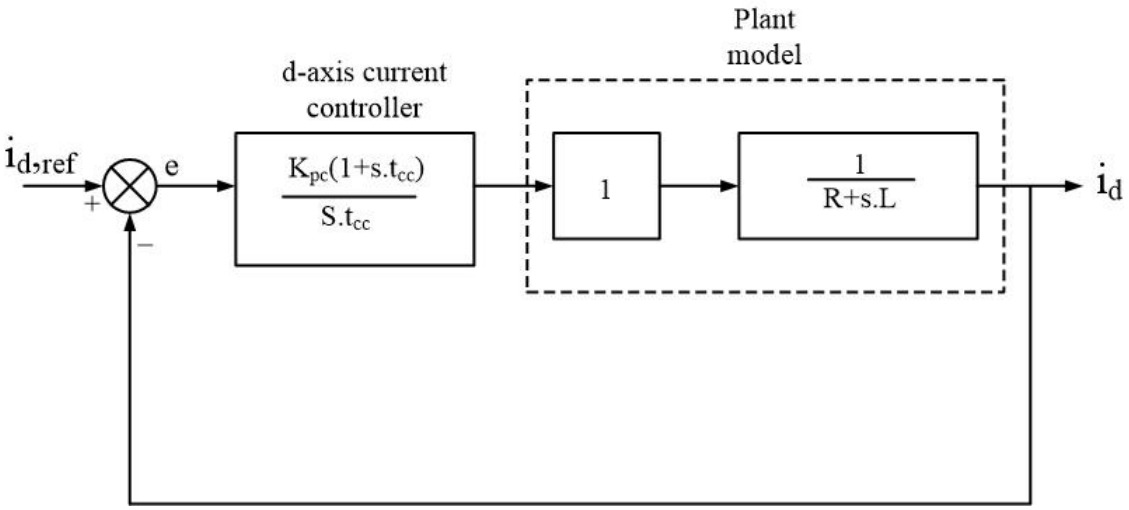

Figure 3.6: Structure of the current control loop

From (3.8), the value of proportional gain k_{pc} (K_p) can be calculated. The value of integral gain (K_i) is calculated from $\frac{k_{pc}}{t_{cc}}$.

3.3.2 Speed controller

The block diagram of the speed controller loop is as shown in Figure. 3.7 The output of the speed PI controller is the reference value of the q-axis current. The current control loop is replaced by its equivalent first order transfer function of bandwidth as designed above. The inverter and speed sensor are treated as constant gain blocks and their dynamics are neglected. The sensor gain is taken as unity.

If the bandwidth of speed controller is chosen as f_{ns}Hz,then

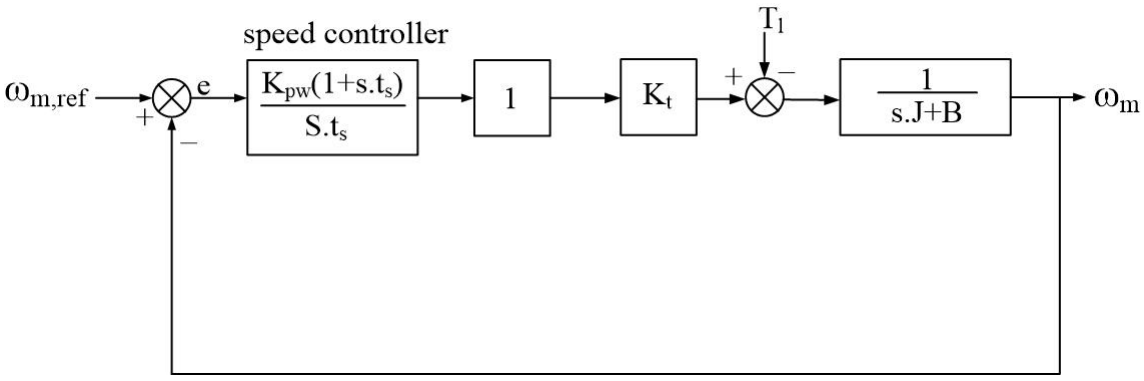

Figure 3.7: Structure of the speed control loop

$$t_{bs} = \frac{1}{2\pi f_{ns}} \tag{3.9}$$

The bandwidth of speed controller loop =$f_{ns} = \frac{1}{10}\times$Bandwidth of current controller

The condition for the loop to have first order response is

$$t_s = \frac{J}{B} \tag{3.10}$$

Therefore, the open loop gain is

$$k_{pw} = \frac{J}{t_{bs}.k_t} \tag{3.11}$$

where k_t is the torque constant.

From the above equation, we can find k_{pw} and the value of integral gain (K_i) is equal to $\frac{k_{pw}}{t_s}$

3.4 SIMULATION RESULTS

The parameters of the BLDC motor used for simulation are shown in Table 3.3. The

Table 3.3: BLDC motor drive parameters used for simulation in FOC

Parameter	Value	Units
Resistance	1.5	ohms
Inductance	4.2	mH
DC Voltage	36	Volts
Moment of Inertia	75	$gmcm^2$
Coefficient of friction	9e-5	$N.m.s$
No.of poles	4	

BLDC motor is started at no-load condition. The speed reference is set to 4000rpm. The three phase currents of the BLDC motor are shown in Figure. 3.8 and the back-emf of the BLDC motor is shown in Figure. 3.9 and the electromagnetic torque of the BLDC motor is shown in Figure. 3.10 and the reference speed and the actual speed of the BLDC motor are shown in Figure. 3.11.

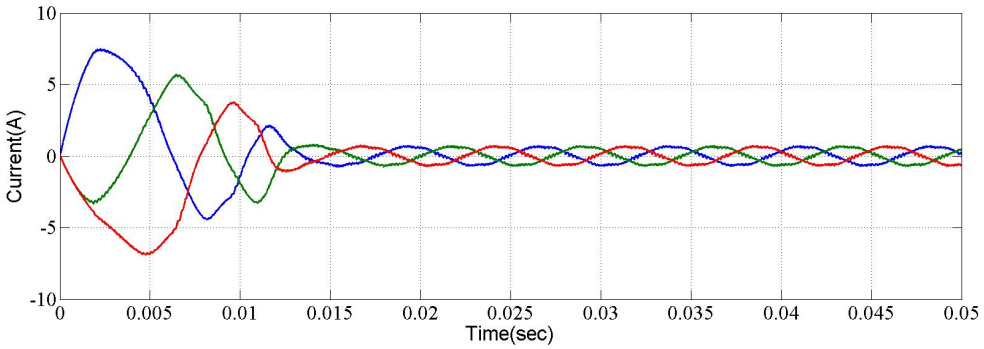

Figure 3.8: The three phase currents under no-load cndition

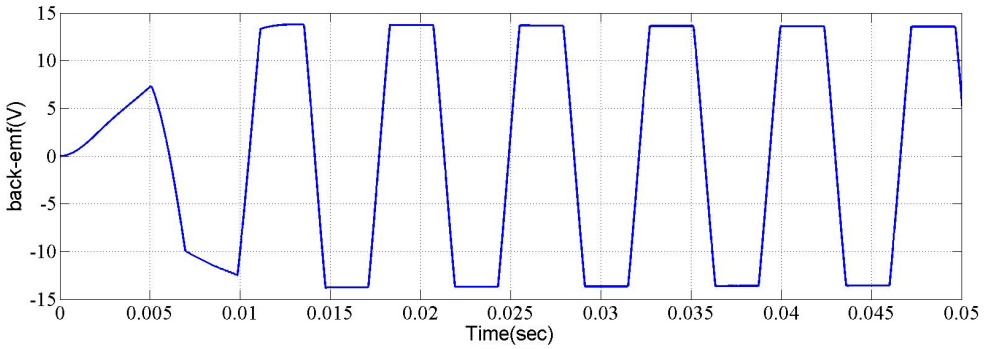

Figure 3.9: The back-emf of BLDC motor

The back-emf generated is 13.15 Volts for the given speed and is trapezoidal in shape. The three phase currents are sinusoidal in shape and have a steady state peak current of 0.7A. From Figure. 3.8 it can be seen that the motor draws a high starting current since there is no induced back-emf.

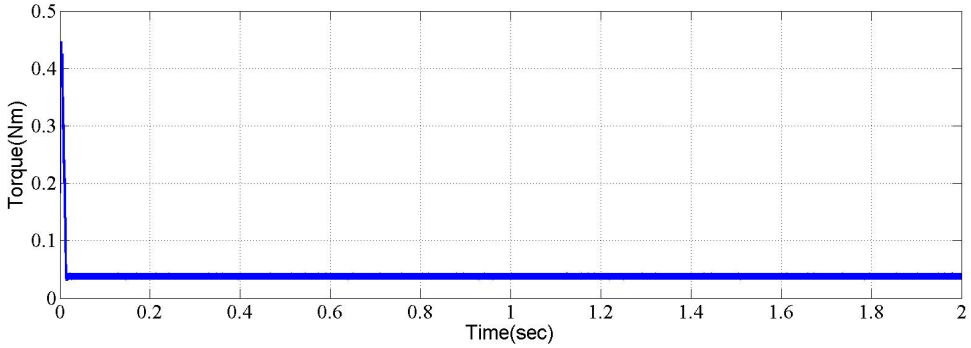

Figure 3.10: Electromagnetic Torque under no-load condition

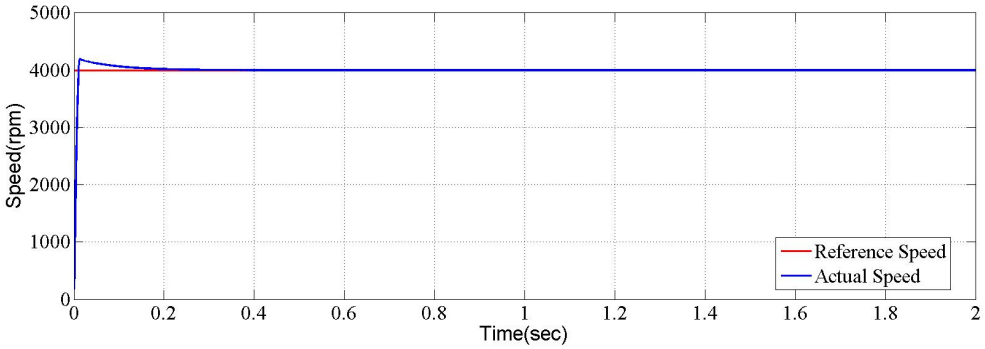

Figure 3.11: Reference Speed and Actual Speed under no-load condition

From Figure. 3.11, it can be seen that the actual speed reached the reference speed at 0.4sec and the speed is constant for entire range. From Figure. 3.10, it is clear that electromagnetic torque equals the load torque within 0.013sec.

3.4.1 Disturbance in load

The BLDC motor is started at no-load condition and rated load torque of 0.11Nm is applied at 2.5sec. The speed is set to 4000rpm.
The phase currents after applying rated load is as shown in Figure. 3.12.

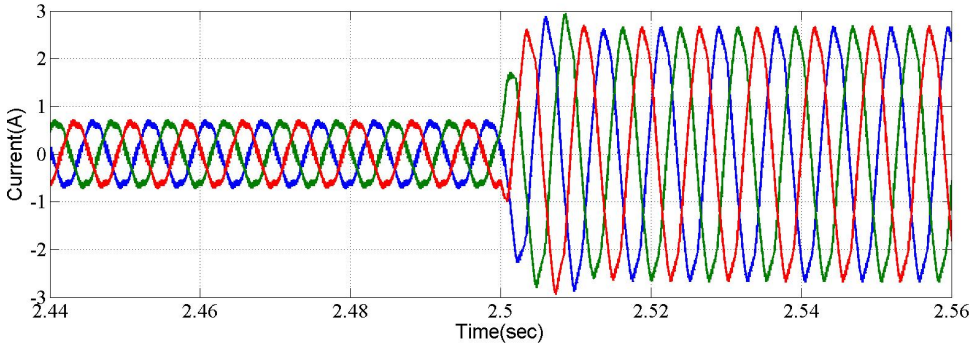

Figure 3.12: The Phase currents during application of load

It can be seen that the steady state load current is sinusoidal in shape with a peak current of 2.7A. The torque and speed waveforms are as shown in Figure. 3.13 and Figure. 3.14 respectively.

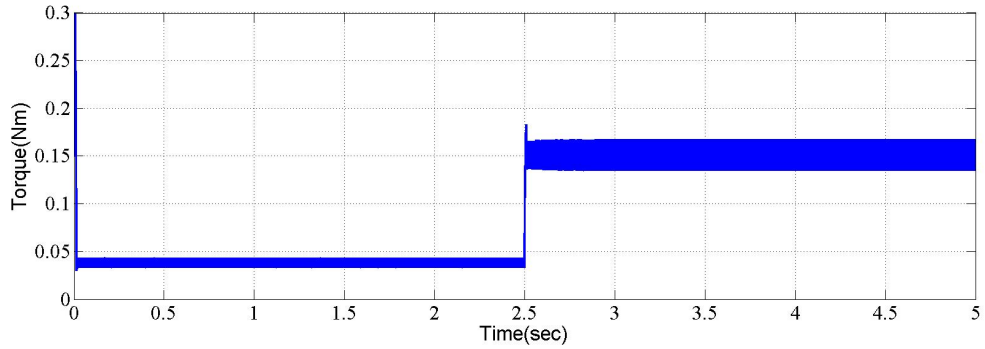

Figure 3.13: Electromagnetic Torque during disturbance in load

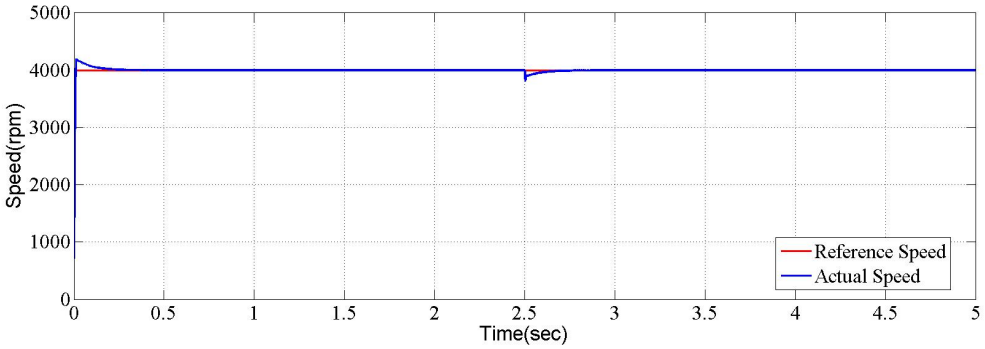

Figure 3.14: Reference speed and Actual speed during disturbance in load

As the load is applied at 2.5sec, from Figure. 3.13, the electromagnetic torque response to the step load torque is instantaneous. From Figure. 3.14, it can be seen that there is a dip in actual speed waveform at the time of disturbance but reached the reference speed at 2.8sec and remained constant in entire range.

3.4.2 Disturbance in speed

The BLDC motor is runned at no-load condition. Initially, the motor is rotated at 4000rpm and at 2.5sec, the reference speed is changed from 4000rpm to 2000rpm. The phase currents at the time of disturbance is shown in Figure. 3.15. The electromagnetic torque during disturbance in speed is as shown in Figure. 3.16. The reference speed and the actual speed at disturbance is as shown in Figure. 3.17.

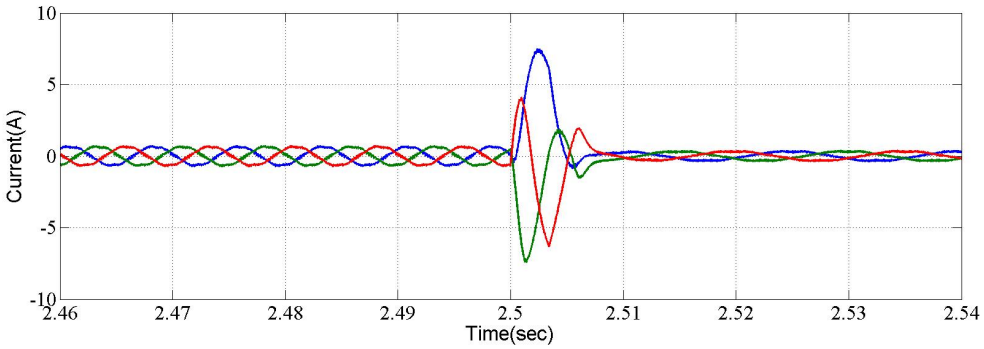

Figure 3.15: Phase currents during speed disturbance)

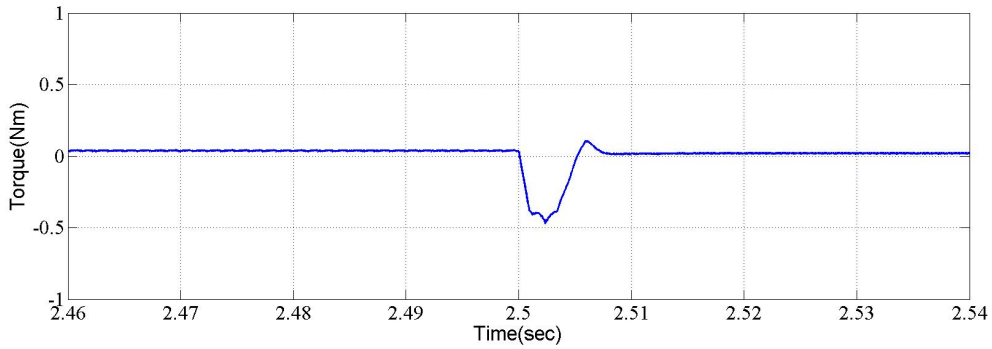

Figure 3.16: Electromagnetic Torque (T_e during speed disturbance)

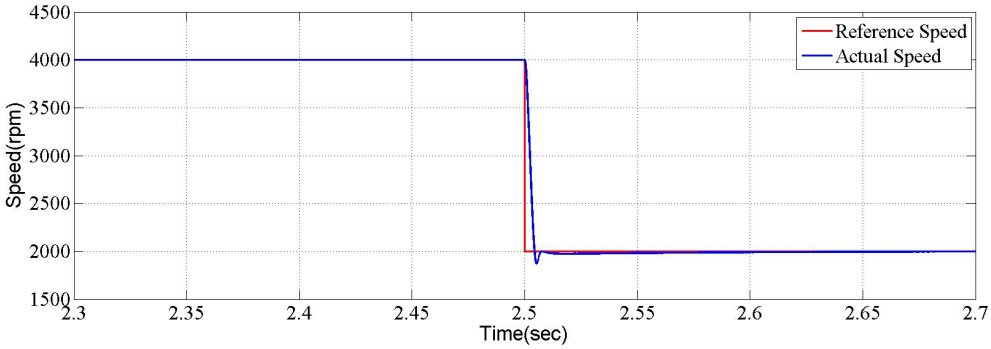

Figure 3.17: Reference speed and actual speed during disturbance

From Figure. 3.17, it can be seen that the actual speed is changing from 4000rpm to 2000rpm and reached steady state at 2.9sec. The motor takes non-zero time to respond for speed change due to momemt of inertia. The electromagnetic torque responds at the time of disturbance and regain its position within 0.008sec.

3.4.3 Speed Reversal

The speed is set to reverse from 4000rpm to -4000rpm at 2.5sec at no-load condition. The torque waveform at the moment of speed reversal is as shown in Figure. 3.18. The

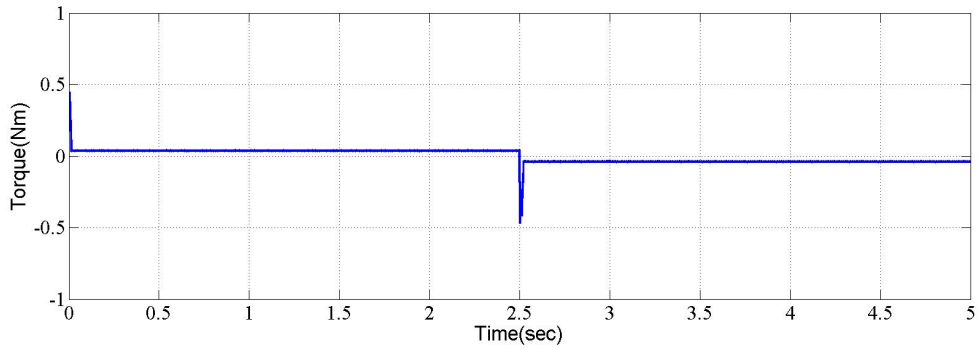

Figure 3.18: Torque (T_e during speed reversal)

phase currents at the time of speed reversal is shown in Figure. 3.19. The waveform of

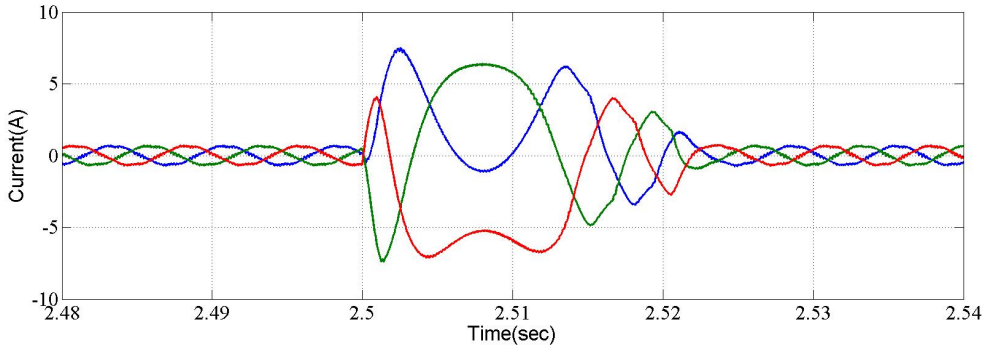

Figure 3.19: The three phase currents during speed reversal

reference speed and actual speed changing from 4000rpm to -4000rpm is as shown in Figure. 3.20.

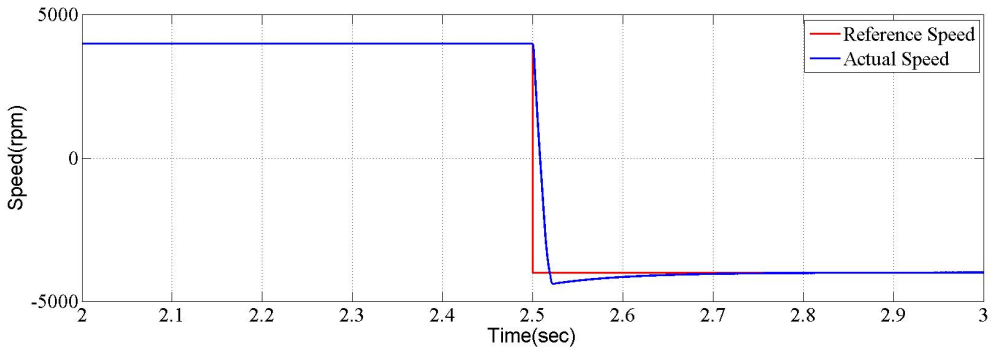

Figure 3.20: Speed reversal

It can be seen that the actual speed is changing from 4000rpm to -4000rpm and reached steady state at 3sec. The motor takes non-zero time for speed change unlike reference speed due to moment of inertia of the motor. The electromagnetic torque responds at the time of disturbance and regain its position within a short time i.e 0.025sec.

CHAPTER 4

CONCLUSIONS AND FUTURE SCOPE

In trapezoidal control, the BLDC motor operates in two phase conduction mode and the currents are quasi-square wave in shape. Due to deviation from ideal conditions related to either the design of motor or the power supplied by the inverter, torque ripples are produced. Because of that, non-ideal current waveforms are injected. In FOC, the electromagnetic torque is controlled independently. Thus, superior control is observed. Starting of motor is very fast and it is able to reach rated speed within short time. The response of the motor to step load torque is instantaneous and the dip in speed during that period is very low. Throughout the operation the speed is almost constant at desired value. The speed reversal is quick and smooth. By using SVPWM, the DC voltage of the inverter is used efficiently. The maximum output voltage based on the SVPWM is 1.15 times bigger than the conventional SPWM.

This simulation work can be further implemented in hardware. The FOC scheme can be implemented without hall sensor information i.e Sensorless FOC as the hall sensors need special mechanical arrangement and are temperature sensitive.

REFERENCES

[1] Fitzgerald, A.E. and Kingsley, C. and Umans, S.D., "*Electric Machinery*,"Tata McGraw-Hill Education, 2002.

[2] Yedale Padmaraja, "*Brushless DC Motor Fundamentals*,"AN885, Microchip Technology Inc, 2003.

[3] D.C. Hanselman, "*Brushless permanent-magnet motor design*,"McGraw-Hill New York, 1994.

[4] P. Pillay and R. Krishnan, "Modelling, simulation, and analysis of permanent-magnet motor drives. II. The brushless DC motor drive," in *IEEE Transactions on Industry Applications*, vol. 25, no. 2, pp. 274-279, Mar/Apr 1989.

[5] Texas Instruments Europe.Field Orientated Control of 3-Phase AC-Motors, *Texas Instruments Application Note, Literature Number*: BPRA073, February, 1998.

[6] P. S. Chaudhari, S. L. Patil and S. K. Pandey, "Application of SVM technique for BLDC motor drive," *2016 IEEE 1st International Conference on Power Electronics, Intelligent Control and Energy Systems (ICPEICES)*, Delhi, 2016, pp. 1-6.